Properties of spin-polarized Pt in magneto-optical Co/Pt multilayered films

Y. P. Lee
Department of Physics, Hanyang University, Seoul 133-791, Korea

R. Gontarz
Institute of Molecular Physics, Polish Academy of Sciences, 60-179 Poznań, Poland

Y. V. Kudryavtsev
Institute of Metal Physics, National Academy of Sciences of Ukraine, 252680, Kiev-142, Ukraine
(Received 4 August 1999; revised manuscript received 14 September 2000; published 5 March 2001)

The magneto-optical and optical properties of the Co/Pt multilayered films (MLF) with a nearly constant Pt sublayer thickness and variable Co sublayer thickness, as well as pure Co and Pt, and $Co_{0.51}Pt_{0.49}$ alloy films have been investigated in the 1.1–4.7-eV energy range experimentally and by solving the multireflection task for various models of MLF. The comparison between experimental and computer-simulated optical properties of the Co/Pt MLF allowed us to evaluate the thickness of the interfacial regions with the alloyed components. The diagonal and off-diagonal components of the optical conductivity tensor were calculated for the spin-polarized Pt layers in the Co/Pt MLF as well as for the pure Co and $Co_{0.51}Pt_{0.49}$ alloy films, and the whole Co/Pt MLF. It was experimentally shown that the structural fcc-$L1_0$ transformation in the $Co_{0.51}Pt_{0.49}$ alloy film caused by an annealing at 610 K for 240 min leads to significant changes in the optical and magneto-optical properties of alloy.

DOI: 10.1103/PhysRevB.63.144402 PACS number(s): 75.70.−i, 78.20.Bh, 78.20.Ls, 78.66.−w

I. INTRODUCTION

The intense study of the magneto-optical (MO) properties of Co/Pt multilayered films (MLF) as well as the Co-Pt alloy films has been performed in recent decade because of the fundamental interests in these systems (for example, the induced magnetic polarization effect in the nonmagnetic Pt sublayers) and of their potential for the practical applications such as storage media. The prominent Kerr rotation in the near ultraviolet (UV) region of these systems is usually attributed to the MO response from the spin-polarized Pt sublayers caused by the exchange splitting of the Pt $5d$ levels. In spite of a huge number of publications devoted to the experimental and theoretical study of these systems (Refs. 1–6 and references therein), and of some attempts to determine the MO properties of the ''magnetic'' Pt, for example, undertaken by Sato and co-workers by analyzing the MO spectra of Fe_xPt_{1-x} alloys,[7] the MO properties of the ''pure'' spin-polarized Pt sublayers have not been extracted confidently yet.

Our knowledge on the MO properties and real structures of the MLF may be verified by a comparison between experimental and computer-simulated MO and optical data, based on an appropriate model for the properties and structures of the constituent sublayers. The use of the bulk MO and optical parameters for the description of the properties of very thin films (a few tenth nm in thickness) is questionable. On the other hand, it has been shown that the experimentally observed MO and optical properties of the $3d$ transition-metal (TM) based MLF are well explained with the electromagnetic wave model employing the bulk optical constants and the MO parameters of the constituent sublayers.[8] For example, according to the results in Ref. 9, the bulk MO and optical properties, and hence the band structures are preserved down to 2.0 nm in thickness. Nevertheless, recent studies of the Co/Au system grown by the molecular-beam epitaxy,[10] ultrathin Co and Fe layers sandwiched by Au,[11,12] and Fe/Zr and Co/Ti MLF (Refs. 13 and 14) provided an evidence that the optical behavior of the ultrathin layers (below a certain ''critical'' thickness) is obviously different from that of the thick film. Atkinson and Dodd also have shown that, for Co/Cu MLF, owing to an increased scattering at the interfaces the bulklike optical constant of Cu the sublayer must be modified by adjusting the relaxation time associated with the conduction electrons in order to explain the experimental spectra.[15]

The origin for the deviation of the optical and MO parameters of the thin metallic sublayers in the MLF from the corresponding bulk values is usually linked with discontinuity, roughness and inhomogeneity of the very thin sublayers. In order to take into account these possible reasons, the modified effective medium theory was employed for describing the MO properties of the Co/Pt MLF.[16]

Some theoretical attempts to interpret the experimental MO data for the Co/Pt MLF had no success without taking into account the interfacial regions.[5] Therefore the idea of existence of the interfaces with the mixed components separating the pure sublayers was employed for interpreting the experimental results for the MLF.[17,18] A reasonable agreement between experimental and simulated MO, and optical data was achieved for various $3d$-TM based MLF by introducing the model of MLF with mixed interfaces and by employing the corresponding bulk MO and optical parameters for the constituent sublayers.[13,14,17,18]

Another quantitative agreement between experimental and modelled Kerr rotation spectra was also achieved by Weller and co-workers[1] for the Co/Pd MLF by solving the equations of the electromagnetic wave theory based on a four-component periodic medium ''Co/interface/Pd/interface,'' where a spin-polarized Pd was chosen for the

TABLE I. The parameters of the investigated Co/Pt MLF. No. is sample number, $d_{Co(Pt)}$ is the measured thicknesses of the Co (Pt) sublayers, and Σ is the total thickness of MLF.

No.	No. of bilayers	d_{Co} (nm)	d_{Pt} (nm)	Σ thickness (nm)	Co content (at. %)
1	50	0.38	1.34	89.0	23.9
2	50	0.46	1.36	90.7	27.3
3	44	0.69	1.25	89.0	38.0
4	40	0.90	1.44	93.5	40.9
5	33	1.89	1.43	109.5	59.4

interface. For these calculations the tabulated optical constants for Co and Pd as well as literature data for the spin-polarized Pd were taken. Nevertheless, such an approach for the Co/Pt MLF failed partly owing to the irrelevant input data. The origin for the discrepancy between experimental and simulated data may originate from an inadequate model for the crystalline structure, and improper use of the optical and MO constants for the constituent sublayers, different from the real ones.

This work is devoted to the determination of the own contribution from the spin-polarized Pt sublayers, induced by a proximity effect with the Co layers, to the total MO response of the Co/Pt MLF by comparing their experimental and computer-simulated MO and optical properties made in the framework of various models for the MLF structure.

The paper is organized as follows: Sec. II contains a brief description of the experimental procedure and the details of the computer simulation, the obtained experimental data and simulation results are analyzed and discussed in Sec. III, and Sec. IV summarizes and concludes the paper.

II. EXPERIMENTAL AND SIMULATION DETAILS

A. Experimental procedure

Co/Pt MLF with a nearly constant Pt sublayer thickness and a variable Co sublayer thickness were prepared onto glass substrates at room temperature (RT) by the computer-controlled double-pair target face-to-face sputtering technique. The parameters of the Co/Pt MLF are presented in Table I. The top layer of all the Co/Pt MLF was Pt.

It is well known that the optical constants of metals depend on their structure, and hence (for the case of thin films) on the deposition conditions. Therefore, in order to secure in the simulation the optical parameters of the constituent sublayers of MLF, $Co_{0.51}Pt_{0.49}$ alloy film as well as pure Co and Pt films of about 100 nm in thickness were also prepared at the same deposition conditions, and their optical properties were measured, too. The as-deposited $Co_{0.51}Pt_{0.49}$ alloy film was cut into two parts and one half was put into a vacuum chamber and annealed at 610 K for 240 min in a high vacuum of 1×10^{-5} Pa. It was shown earlier[19] that such a preparation conditions allow us to obtain the $Co_{0.51}Pt_{0.49}$ alloy films in a disordered state with the fcc lattice (as-deposited sample) and in the ordered tetragonal phase of AuCu I ($L1_0$) type with $c/a=0.974$ (annealed sample). The details of the relevant sample preparation and structural analysis can be found elsewhere.[5,19]

The field dependence of magnetization for the Co/Pt MLF was measured using a vibrating sample magnetometer (VSM) at RT in a magnetic field up to 1.0 T for an in-plane geometry. The optical properties (the real and imaginary parts of the complex refractive index, $\tilde{N}=n-ik$) of the samples were measured at RT in a spectral range of 260–1130 nm (4.7–1.1 eV) at a fixed incidence angle of 73° by the polarimetric Beattie technique.[20] The obtained values of n and k were used for calculating the spectral dependence of the real (ε_1) and imaginary (ε_2) parts of the diagonal components of the dielectric function (DF) (for polycrystalline films, $\tilde{\varepsilon}_{xx}=\tilde{\varepsilon}_{yy}=\tilde{\varepsilon}_{zz}=\varepsilon_1-i\varepsilon_2$), and also of the optical conductivity [OC: (σ)] by using the expressions: $\varepsilon_1=n^2-k^2$, $\varepsilon_2=2nk$, and $\sigma(\hbar\omega)=\varepsilon_2\omega/4\pi$, where ω is the angular frequency of light.

The MO equatorial Kerr effect (EKE) of the Co/Pt MLF, and $Co_{0.51}Pt_{0.49}$ alloy and pure Co films was measured at RT by the dynamical method using the p-plane polarized light at two angles of incidence (66 and 75°) in a spectral range of 260–1130 nm (4.7–1.1 eV) and in an ac magnetic field of 3 kOe. The EKE value, $\delta_p=\Delta I/I_o$, is the relative change in intensity of the reflected light, caused by the magnetization of the sample in an external magnetic field directed transversely to the plane of the light incidence. The real (ε_2') and imaginary (ε_1') parts of the off-diagonal components of the DF ($\tilde{\varepsilon}_{xy}=-\tilde{\varepsilon}_{yx}=i\tilde{\varepsilon}',\tilde{\varepsilon}'=\varepsilon_1'-i\varepsilon_2'$) for the investigated samples were determined by using the algorithm in Ref. 20 and the experimental results of the optical study and the MO measurements at two angles of incidence.

B. Simulation details

It is well known that the skin penetration depth in metals depends on their optical properties and ω, and is about 20 nm for most metals. Therefore it is clear that, in our case, the reflected electromagnetic wave from the surface of MLF carries information on about ten surface sublayers. The theoretical simulations of δ_p, σ, and ε_1 spectra for the Co/Pt MLF were performed by solving exactly a multireflection problem by using the scattering matrix approach,[22] assuming either ''sharp'' (ideal) interfaces resulting in rectangular depth profiles of the components or ''mixed'' (alloylike) interfaces of variable thickness between pure metal sublayers. The number of the constituent sublayers, their nominal thickness and optical properties, and also the angle of incidence were the input parameters for the simulation. The measured optical and MO parameters of thick (bulklike) pure Co and Pt films, and the $Co_{0.51}Pt_{0.49}$ alloy films were also employed in these simulations.

It should also be noted that the sharp interface between sublayers is considered as the ideal case, and the mixed interface seems to us more probable. In case of the mixed interfaces, the transition from the Co to Pt sublayer encounters a transitional region where the Co_xPt_{1-x} alloy concentration is gradually changed from a Co-rich Co_xPt_{1-x} alloy to a Pt-rich Co_xPt_{1-x} alloy through the equiatomic CoPt. In other words, such an interfacial region can be expressed by a

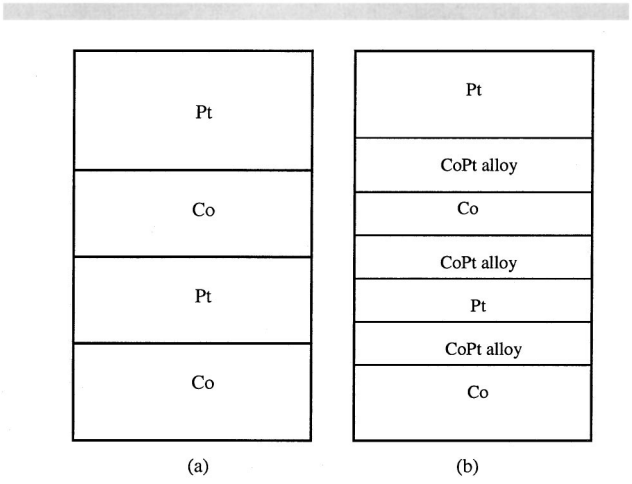

FIG. 1. Models of Co/Pt MLF with (a) sharp and (b) mixed interfaces, which were used in the simulations.

set of Co_xPt_{1-x} alloy planes with different compositions. On the other hand, the thickness of this interfacial region cannot be larger than a half of the bilayer period, and is usually around 1 nm. For example, Co/Zr MLF turn out to have an interfacial region of 0.8 and 1.2 nm for a bilayer period of 6.7 and 9.7 nm, respectively, and Fe/Zr MLF also show an interfacial thickness of 1.0 nm or less in the case of a bilayer period of 5.2 nm.[13] In addition, the alloys of one or two monolayers thick have no significant physical meaning for the relevant properties. Therefore the equiatomic CoPt alloy is considered as an idealized approximation representing the actual interface structure and simplifying the simulation of the optical and MO properties of the Co/Pt MLF with mixed interfaces. The models which were used in the simulations of the optical and MO properties of the Co/Pt MLF are sketched in Fig. 1.

The complex DF $\hat{\varepsilon}$ for a magnetic medium magnetized along z axis with threefold or higher symmetry about z axis has the following form:

$$\hat{\varepsilon}=\begin{pmatrix} \tilde{\varepsilon}_{xx} & \tilde{\varepsilon}_{xy} & 0 \\ -\tilde{\varepsilon}_{xy} & \tilde{\varepsilon}_{yy} & 0 \\ 0 & 0 & \tilde{\varepsilon}_{zz} \end{pmatrix}, \tag{1}$$

where, in general, the diagonal and off-diagonal terms are complex. Introducing the complex Voigt parameter

$$\tilde{Q}=\frac{i\tilde{\varepsilon}_{xy}}{\tilde{\varepsilon}_{xx}} \tag{2}$$

and assuming that, for polycrystalline materials, $\tilde{\varepsilon}_{xx}=\tilde{\varepsilon}_{yy}=\tilde{\varepsilon}_{zz}$, $\tilde{\varepsilon}_{xy}=i\tilde{\varepsilon}_{xx}\tilde{Q}$; $\tilde{Q}=Q_1-iQ_2$, we obtain

$$\hat{\varepsilon}=\tilde{\varepsilon}_{xx}\begin{pmatrix} 1 & -i\tilde{Q} & 0 \\ i\tilde{Q} & 1 & 0 \\ 0 & 0 & 1 \end{pmatrix}. \tag{3}$$

For a magnetically ordered medium in a magnetic field, the complex refractive indices for the left$(-)$- and right $(+)$-circularly polarized light can be defined as

$$\tilde{N}_{\pm}^2=\tilde{\varepsilon}_{xx}\pm i\tilde{\varepsilon}_{xy}=\tilde{\varepsilon}_{xx}(1\mp\tilde{Q}), \tag{4}$$

while, for a nonmagnetic medium, this expression can be transformed into

$$\tilde{N}^2=\tilde{\varepsilon}_{xx}=\varepsilon_1-i\varepsilon_2=(n-ik)^2=(n^2-k^2)+i2nk. \tag{5}$$

C. Optical properties of the MLF

Let us consider the MLF consisting of $1,2,3,\ldots,j,\ldots,m$ parallel, isotropic, and homogeneous layers which are put between a semiinfinite ambient medium (0) and a substrate $(m+1)$. The complex refractive indices of the medium and substrate are N_0 and N_{m+1}, respectively. Let $E^+(z)$ and $E^-(z)$ are the complex amplitudes of the electromagnetic wave which propagates forward and back in an arbitrary plane z. E for different planes z' and z'' must be connected by the reorganization

$$\begin{pmatrix} E^+(z') \\ E^-(z') \end{pmatrix}=\begin{pmatrix} S_{11} & S_{12} \\ S_{21} & S_{22} \end{pmatrix}\times\begin{pmatrix} E^+(z'') \\ E^-(z'') \end{pmatrix}, \tag{6}$$

or, in a shorter way, Eq. (6) can be rewritten as

$$E(z')=SE(z''), \tag{7}$$

where S is the so-called scattering matrix

$$S=\begin{pmatrix} S_{11} & S_{12} \\ S_{21} & S_{22} \end{pmatrix}. \tag{8}$$

The scattering matrix S for such a MLF can be expressed as a result of the multiplication of the reflection and phase matrices, I and F, respectively, for each boundary and layer, respectively

$$S=I_{01}F_1I_{12}F_2\cdots I_{j(j+1)}F_j\cdots I_{m(m+1)}F_{m+1}. \tag{9}$$

The reflection matrix $I_{j(j+1)}$ describes the reflection between jth and $(j+1)$th adjacent layers,

$$I_{j(j+1)}=\frac{1}{T_{j(j+1)}}\begin{pmatrix} 1 & R_{j(j+1)} \\ R_{j(j+1)} & 1 \end{pmatrix}, \tag{10}$$

where the Fresnel coefficients of reflection and transmission between j and $j+1$ boundaries, $R_{j(j+1)}$ and $T_{j(j+1)}$, respectively, are calculated for the p and s polarizations by using the complex refraction index for jth layer, $\tilde{N}_j=n_j-ik_j$;

$$R_{j(j+1)}^p=\frac{\tilde{N}_j^2\tilde{A}_{j+1}-\tilde{N}_{j+1}^2\tilde{A}_j}{\tilde{N}_j^2\tilde{A}_{j+1}+\tilde{N}_{j+1}^2\tilde{A}_j},\quad T_{j(j+1)}^p=\frac{2\tilde{N}_j\tilde{N}_{j+1}\tilde{A}_{j+1}}{\tilde{N}_j^2\tilde{A}_{j+1}+\tilde{N}_{j+1}^2\tilde{A}_j}, \tag{11}$$

and

$$R_{j(j+1)}^s=\frac{\tilde{A}_{j+1}-\tilde{A}_j}{\tilde{A}_{j+1}+\tilde{A}_j},\quad T_{j(j+1)}^s=\frac{2\tilde{A}_{j+1}}{\tilde{A}_{j+1}+\tilde{A}_j}, \tag{12}$$

where $\tilde{A}_j = \sqrt{\tilde{N}_j^2 - \sin\varphi}$ and φ is the angle of incidence.

The phase matrix F_j for the jth layer can be defined as

$$F_j = \begin{pmatrix} e^{i\delta_j} & 0 \\ 0 & e^{-i\delta_j} \end{pmatrix}, \tag{13}$$

where $2\delta_j = 4\pi(d_j/\lambda)\tilde{N}_j \cos\varphi_j$, d_j is the thickness of the jth sublayer, and λ is the light wavelength. Thus it is clear that the knowledge about the optical constants of each layer, the thickness and the angle of incidence are enough for calculating the resultant scattering matrix for the whole MLF.

After matrix S being calculated, the ellipsometric angles, Ψ and Δ, for the whole MLF (as if the material is actually homogeneous) could be obtained by using the main equation of ellipsometry

$$\tan\Psi \times e^{i\Delta} = \frac{S_{21}^p}{S_{11}^p} \times \frac{S_{11}^s}{S_{21}^s}. \tag{14}$$

While the ellipsometric angles are determined by using Eq. (14), the effective optical constants, $n_{(eff)}$ and $k_{(eff)}$ for the whole MLF can be calculated from the equations for the optical invariants,

$$\varepsilon_{1(eff)} = n_{(eff)}^2 - k_{(eff)}^2 = \sin\varphi \times \left[1 + \tan^2\varphi \frac{\cos^2 2\Psi - \sin^2 2\Psi \sin^2\Delta}{(1 - \sin 2\Psi \cos\Delta)^2} \right], \tag{15}$$

and

$$\varepsilon_{2(eff)} = 2 n_{(eff)} k_{(eff)} = 2 \sin^2\varphi \tan^2\varphi \times \left[\frac{\cos 2\Psi \times \sin 2\Psi \times \sin\Delta}{(1 - \sin 2\Psi \times \cos\Delta)^2} \right]. \tag{16}$$

D. Magneto-optical properties of the MLF

According to Eq. (4), the complex refractive indices of each layer for the right- and left-circularly polarized light can be defined as

$$\tilde{N}_{+j}^2 = \tilde{\varepsilon}_{xxj}(1 - \tilde{Q}_j), \tag{17}$$

$$\tilde{N}_{-j}^2 = \tilde{\varepsilon}_{xxj}(1 + \tilde{Q}_j). \tag{18}$$

Using the same formalism, which was employed for the determination of the effective optical constants for the whole MLF, and Eqs. (17) and (18), the effective complex refractive indices for the left- and right-circularly polarized light can be determined, and then the effective diagonal and off-diagonal components of the DF can be also obtained:

$$\tilde{\varepsilon}_{xx(eff)} = \frac{N_{(eff)+}^2 + N_{(eff)-}^2}{2}, \tag{19}$$

$$Q_{(eff)} = \frac{N_{(eff)+}^2 - N_{(eff)-}^2}{N_{(eff)+}^2 + N_{(eff)-}^2}, \tag{20}$$

$$\tilde{\varepsilon}_{xy(eff)} = -i\tilde{\varepsilon}_{xx(eff)}\tilde{Q}_{(eff)} = \tag{21}$$

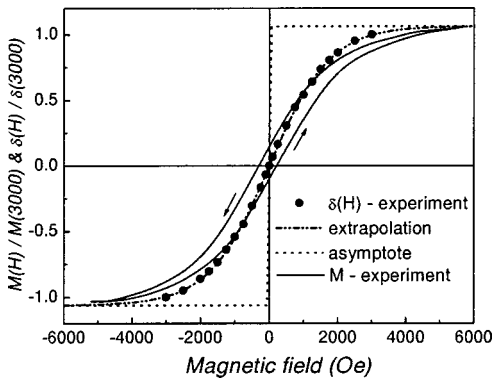

FIG. 2. Extrapolation (dash-dot-dot) to the saturation level (dot) of the experimental $\delta_p(H)$ dependence for sample 4 (circles), together with the magnetization loop (solid) obtained by VSM.

$$\varepsilon'_{1(eff)} - i\varepsilon'_{2(eff)} = \frac{N_{(eff)+}^2 - N_{(eff)-}^2}{2}. \tag{22}$$

The transverse or equatorial Kerr effect for the whole MLF can be expressed as[21]

$$\delta_p = 2\sin 2\varphi \times \left(\frac{A \times \varepsilon'_{1(eff)}}{A^2 + B^2} + \frac{B \times \varepsilon'_{2(eff)}}{A^2 + B^2} \right), \tag{23}$$

where

$$A = \varepsilon_{2(eff)} \times (2\varepsilon_{1(eff)} \times \cos^2\varphi - 1),$$

$$B = (\varepsilon_{2(eff)}^2 - \varepsilon_{1(eff)}^2) \times \cos^2\varphi + \varepsilon_{1(eff)} - \sin^2\varphi.$$

III. RESULTS AND DISCUSSION

Figure 2 presents the magnetization loop, together with the magnetic-field dependence of the MO response for sample 4. It is seen that an ac magnetic field of 3 kOe (the maximum field available to us) is not enough to saturate the MO effect. The other investigated Co/Pt MLF exhibit nearly the same field dependence of δ_p, but with a different asymptote. Therefore the saturated values of the EKE for the investigated Co/Pt MLF were determined as the asymptotic limit of the extrapolated experimental $\delta_p(H)$ data. Then, the raw experimental $\delta_p(\hbar\omega)$ dependencies at $H = 3$ kOe for all the investigated Co/Pt MLF were artificially ''saturated'' by multiplying the corresponding ''saturating'' factors. These factors lay between 1.038 and 1.165. Such a significant ac magnetic field necessary for the in-plane saturation of δ_p allows us to suppose the existence of a remarkable perpendicular magnetic anisotropy in the investigated Co/Pt MLF.

Figure 3 shows the experimental EKE spectra for the Co/Pt MLF at $\varphi = 66°$. The EKE spectrum for a pure Co film is also shown for the comparison, which exhibits a small maximum (or shoulder) near 1.6–1.7 eV and an intense peak near 4.25 eV. It should be mentioned here that the obtained results for the Co film are in a reasonable agreement in peak position and intensity with the corresponding data for the crystalline bulk as well as for the thin amorphous film.[23,24] In general, the EKE spectra for the investigated Co/Pt MLF conserve the shape of the Co spectrum. Furthermore, in the

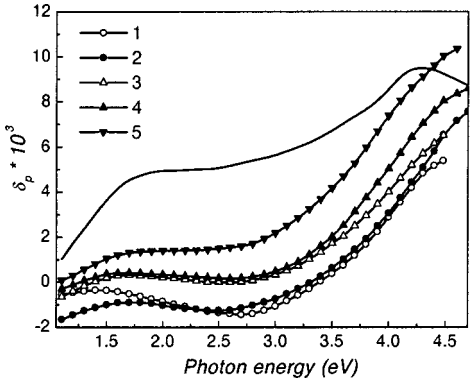

FIG. 3. Experimental EKE spectra for the Co/Pt MLF at $\varphi = 66°$. The EKE spectrum for a pure Co film is also shown by solid line for the comparison.

visible and near infrared (IR) regions of the spectra ($\hbar\omega < 3$ eV), the EKE values for the Co/Pt MLF are nearly proportional to the Co content in the film, while this correspondence is disturbed in the UV region: the values of δ_p for the Co/Pt MLF are nearly the same as for the Co film or even higher. The similar behavior was also observed for the as-deposited and annealed $Co_{0.51}Pt_{0.49}$ alloy films (see Fig. 4). It should be mentioned here that the EKE spectra for two structural states of the alloy films are noticeably different, exhibiting a prominent influence of the local environment on the MO response of the alloy.

Figures 5 and 6 present the experimental σ and ε_1 spectra for the investigated Co/Pt MLF and the $Co_{0.51}Pt_{0.49}$ alloy film, respectively, both together with the spectra for the pure Co and Pt films. The optical conductivity for both Co and Pt films gradually increases with decreasing photon energy, revealing a small shoulder near 1.8 eV for the Co film. In general, the experimental σ spectra for the Co and Pt films agree with other experimental results on the bulk and thin-film samples.[25–28] According to the theoretical calculations of the electronic structure and optical properties of Co, the main optical absorption is due to the electron excitations within minority-spin subbands.[29] It should be mentioned here that σ (and hence ε_2) for the Pt films is larger than the Co film in the whole investigated spectral range. Nearly the

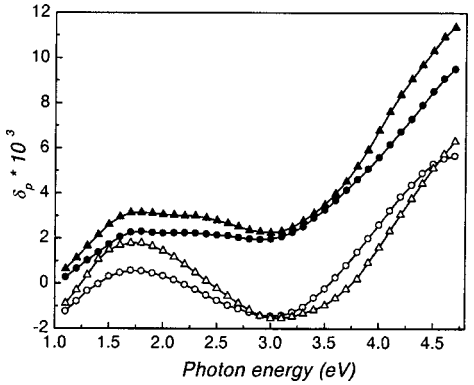

FIG. 4. Experimental EKE spectra for the as-deposited (circles) and annealed (triangles) $Co_{0.51}Pt_{0.49}$ alloy films at $\varphi = 66°$ (solid symbols) and $\varphi = 75°$ (open).

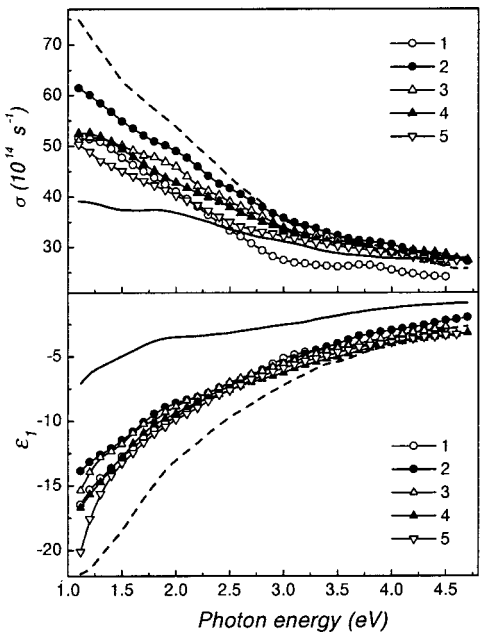

FIG. 5. Experimental (a) σ and (b) ε_1 spectra for the Co/Pt MLF. The corresponding σ and ε_1 spectra for pure Co and Pt films are shown by solid and dashed lines, respectively.

same regularities are also observed for the experimental spectra of the real parts of the diagonal components of the DF for the Co and Pt films: the $\varepsilon_1(\hbar\omega)$ values for both films increase in absolute value with decreasing photon energy, being negative in the whole spectral range. Thus it can be concluded that the absolute values of ε_1 and ε_2 for the Pt

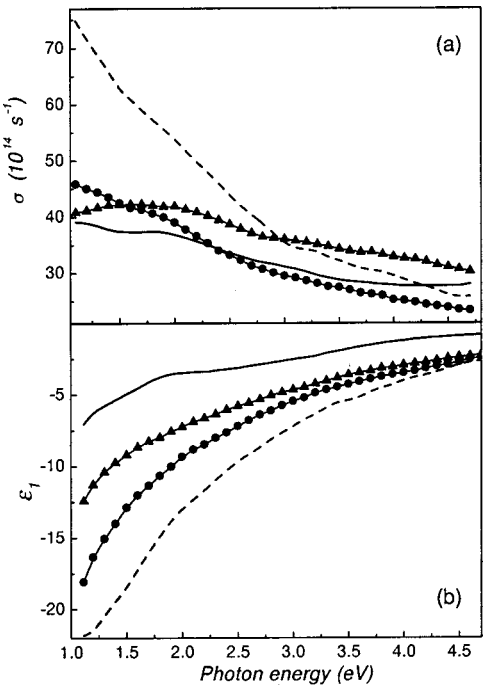

FIG. 6. Experimental (a) σ and (b) ε_1 spectra for the as-deposited (circles) and annealed (triangles) $Co_{0.51}Pt_{0.49}$ alloy films. The corresponding σ and ε_1 spectra for pure Co and Pt films are shown by solid and dashed lines, respectively.

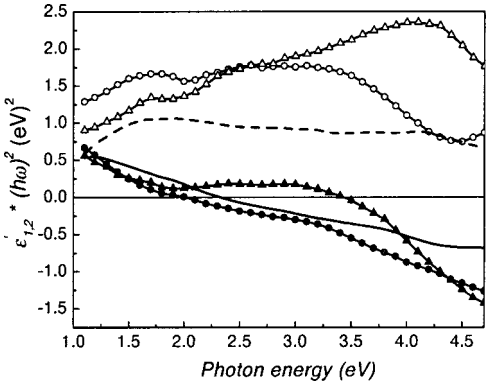

FIG. 7. Calculated $\varepsilon_1' \times (\hbar\omega)^2$ (solid circles, solid triangles and solid line) and $\varepsilon_2' \times (\hbar\omega)^2$ (open circles, open triangles and dashed line) spectra for pure Co film (solid and dashed lines), and the as-deposited (solid and open circles) and annealed (solid and open triangles) $Co_{0.51}Pt_{0.49}$ alloy films.

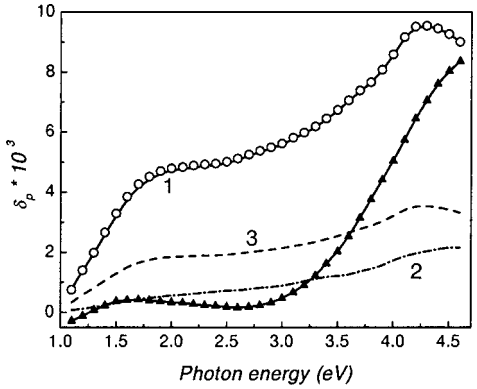

FIG. 8. Simulated (for the case of sharp interfaces) EKE spectra at $\varphi = 66°$ for hypothetical $40\times$(0.90 nm Co/1.44 nm Sp) MLF, where Sp is the ferromagnetic Co (''1''), nonferromagnetic Pt (''2''), or nonferromagnetic Co (''3''). The experimental EKE spectra for pure Co film (circles) and sample 4 (solid triangles) are also shown for the comparison.

film are always larger in the investigated energy region than the corresponding ones for the Co film. In general, the experimental $\sigma(\hbar\omega)$ and $\varepsilon_1(\hbar\omega)$ spectra for the Co/Pt MLF lie between the limits marked by the corresponding dependences for the Pt and Co films, nearly showing the proportionality to the Co (or Pt) content in the MLF (see Fig. 5). On the other hand, the $\sigma(\hbar\omega)$ and $\varepsilon_1(\hbar\omega)$ spectra for the $Co_{0.51}Pt_{0.49}$ alloy films, in spite of belonging again to the regions set by the Co and Pt borders, manifest the noticeable dependence on the structural state of alloy (see Fig. 6).

For the simulation of the MO properties for the Co/Pt MLF with mixed (alloylike) interfaces between pure Co and Pt sublayers, the off-diagonal components of the DF for Co and CoPt alloy must be determined. Figure 7 shows the calculated $\varepsilon_1' \times (\hbar\omega)^2$ and $\varepsilon_2' \times (\hbar\omega)^2$ spectra for the pure Co and $Co_{0.51}Pt_{0.49}$ alloy films. The same calculations have been also performed for all the investigated Co/Pt MLF.

The MO properties of pure Co have been investigated experimentally and theoretically.[5,23,29–34] The obtained results for the pure Co film in the present work show an excellent agreement with published data. It is seen in Fig. 6 that the $\varepsilon_2' \times (\hbar\omega)^2$ spectrum for the Co film shows two tiny features near 1.6 and 4.2 eV and a wide plateau between them. According to Uba *et al.*,[5] or Uspenskij and Khalilov,[29] these peaks should be located at 1.7 or 1.5 eV and 4.2 or 4.3 eV, respectively. The dispersive part of the off-diagonal component for the DF, $\varepsilon_1' \times (\hbar\omega)^2$, for the Co film decreases gradually with photon energy, intersecting the zero line near 2.2 eV.

First of all, it is necessary to emphasize that the $\varepsilon_{1,2}' \times (\hbar\omega)^2$ spectra for both structural states of the $Co_{0.51}Pt_{0.49}$ alloy film are significantly different. Such a behavior exhibits an influence of the local environment on the spectral shape and value of the MO effect of this alloy. The high structural sensitivity of the MO effect for FePt and CoPd alloys was also observed.[35–37] The $\varepsilon_2' \times (\hbar\omega)^2$ spectrum for the as-deposited $Co_{0.51}Pt_{0.49}$ alloy film reveals a prominent peak near 1.7 eV and a wide intense absorption peak in the visible region. The transition from the fcc to ordered $L1_0$ phase leads to a reduced intensity of the low-energy peak and also to a significant increase in a magnitude of the main peak with a shift to the higher energy side. The noticeable changes are also observed in the $\varepsilon_1' \times (\hbar\omega)^2$ spectra: the structural ordering causes the formation of a wide maximum near 3 eV. The obtained experimental spectra agree with results of the first-principles calculations. According to the theoretical results of Uba and co-workers,[5] the absorptive part of the off-diagonal component of the DF for CoPt alloy exhibits an intense absorption, whose magnitude is twice larger with respect to Co in the UV region. The dominant contribution to the $\varepsilon_2' \times (\hbar\omega)^2$ in the 1–6 eV region comes from transitions to the unoccupied states lying in a rather narrow energy interval of $\sim$1 eV just above E_F. These states are formed by the strongly hybridized Co *d* and Pt *d* electrons.

In order to test the software and the simulation process, the EKE spectra for hypothetical MLF, which consists of ferromagnetic Co layers and spacer (Sp) layers (ferromagnetic Co, nonmagnetic Co or nonmagnetic Pt), and which have the same nominal structure as the sample 4, i.e., 40 $\times$(0.90 nm Co/1.44 nm Sp), were calculated for the case of sharp interfaces. The results are shown in Fig. 8, together with the experimental EKE spectra for the pure Co film and the Co/Pt MLF (sample 4). It is an evidence for the correct simulation process that the EKE spectrum for the pure Co film coincides with the simulation with the ferromagnetic Co as the spacer (actually, a pure Co film of 93.5 nm in thickness). It is also seen that the simulated δ_p spectrum with the nonmagnetic Pt spacers (curve 2 in Fig. 8) has about of a half of the intensity for the simulation with the nonmagnetic Co spacers (curve 3 in Fig. 8). This clearly shows an interplay of the optical parameters of the constituent sublayers on the resultant δ_p for the MLF. Apparently, because the real and imaginary parts of the DF for pure Pt are larger with respect to pure Co, the effective ε_1 and ε_2 in the case of nonmagnetic Pt spacers become bigger compared with the case of nonmagnetic Co spacers. According to Eq. (23), the increase in the effective ε_1 and ε_2 should lead to a decrease in δ_p.

The intensity of the simulated EKE spectra for all the investigated Co/Pt MLF (based on the sharp interfaces and

nonmagnetic Pt sublayers) increase with the overall Co content in the MLF, repeating the experimentally observed regularities. In the visible and near IR region of spectra ($\hbar\omega < 3$ eV) the magnitudes of the experimental and simulated EKE spectra are comparable, while in the UV region the discrepancy between them increases with photon energy: the experimental δ_p for all the investigated Co/Pt MLF exceed the simulated ones. This is clearly illustrated in Fig. 8 for sample 4. Naturally, the origin of such a significant discrepancy connected with the appearance of additional contributions to the resultant MO response of the Co/Pt MLF. This effect might be explained by the optical interference.[38] However, we believe that the interference effect could not be responsible for the additional MO response in the UV region, because the optical wave path at the employed angles of incidence is much shorter than the wavelength in the whole spectral range.

Usually such an additional contribution to the resultant MO response of the Co/Pt MLF is thought to be attributed to the spin-polarized Pt sublayers.[1] On the other hand, the interfaces between pure Co and Pt sublayers in the real Co/Pt MLF is not ideal, other sources for the additional contribution to the resulting MO response from Co/Pt MLF should be considered. As evidently seen in Fig. 4, the $Co_{0.51}Pt_{0.49}$ alloy films exhibit a prominent EKE whose magnitude is even higher than δ_p for the Co/Pt MLF. Therefore an additional contribution to the resultant MO response of the Co/Pt MLF seems to be probable from the alloylike interfacial regions.

The uncertainty in the determination of the sources can be reduced by performing the simulations of the optical properties of the Co/Pt MLF. These simulations may allow us to determine the real structure of the Co/Pt MLF. The thickness of the mixed interfaces in these simulations was considered as a variable parameter and was chosen in order to obtain the best coincidence between experimental and simulated optical properties for all the investigated Co/Pt MLF. Figure 9 presents (as an example) the simulated optical properties for one (sample 5) of the investigated Co/Pt MLF. The aforementioned structure models were employed: sharp interfaces, and mixed interfaces of variable thickness. The optical properties of the mixed interfaces were approximated by those of the as-deposited and annealed $Co_{0.51}Pt_{0.49}$ alloy films. It is noticed again that the optical properties of the $Co_{0.51}Pt_{0.49}$ alloy films depend significantly on the alloy structure as clearly seen in Fig. 6. Because of a possible oxidation of the Co/Pt MLF, which can lead to some parallel downward shift of the experimental ε_2 spectra, the focus was given to obtain the best agreements in shape between of the both experimental and modelled σ, and ε_1 spectra.

Even though the complete coincidence was not reached, it can be concluded that the model of MLF with mixed interfaces of 0.5, 0.9, and 1.0 nm in thickness for samples 3, 4, and 5, respectively, offers the closest approximation to the experimental data. The estimated thicknesses of the mixed interfaces are in a reasonable agreement with a estimation made by Angelakeris and co-workers for the Co/Pt MLF prepared by a dual electron-beam evaporation in a UHV condition.[17] It can be also supposed that observed slight discrepancies between experimental and best-simulated σ, and

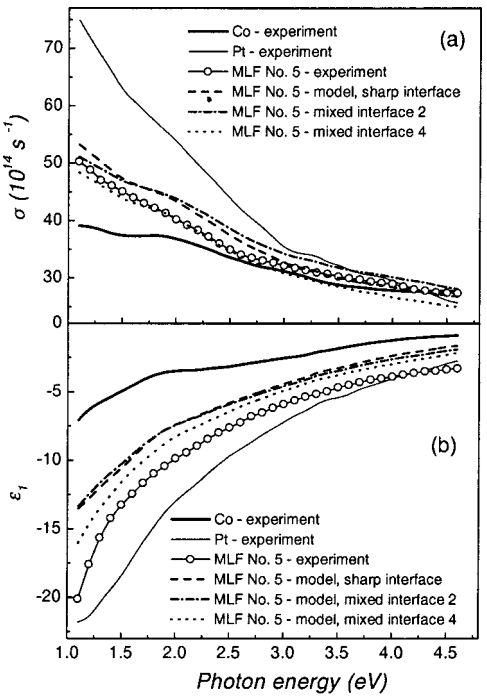

FIG. 9. Simulated (a) σ and (b) ε_1 spectra for the 33 $\times$(1.89 nm Co/1.43 nm Pt) MLF (sample 5). The mixed interfaces of 5 (''1,'' ''2'') and 10 (''3,'' ''4'') in thickness were modelled by employing the optical constants of the as-deposited (''1,'' ''3'') and annealed (''2,'' ''4'') $Co_{0.51}Pt_{0.49}$ alloy films. Only ''2'' and ''4'' are presented to avoid the confusion due to a crowd of data. The corresponding experimental spectra (circles) as well as those for pure Co (solid line) and Pt (thin solid line) films are also shown for the comparison.

ε_1 spectra for the Co/Pt MLF originate from a more complicated structure of the real interfaces and/or thickness dependence of the optical constants.

In order to determine the additional (in the comparison with the simulation) MO contribution of the Co/Pt MLF, we applied the same approach as was employed for the calculation of the off-diagonal components for the pure Co and $Co_{0.51}Pt_{0.49}$ alloy films. First of all, the differences between experimental and simulated (for the case of mixed interfaces) EKE spectra of the Co/Pt MLF at two angles of incidence were determined. In this case the additional contribution arises mainly from the spin-polarized Pt sublayers. Thus we can estimate the lower and upper limits for the MO properties of the spin-polarized Pt sublayers in the investigated Co/Pt MLF.

In this way, we obtained the $\varepsilon_1' \times (\hbar\omega)^2$ and $\varepsilon_2' \times (\hbar\omega)^2$ spectra attributed to the spin-polarized Pt sublayers, as shown in Figs. 10 and 11. It is seen that these spectra exhibit a rather general behavior: the absorptive part of the off-diagonal components of the DF, the $\varepsilon_2' \times (\hbar\omega)^2$ spectra, show two prominent peaks near 1.3 and 4 eV, and also a few tiny peculiarities in the visible region, while the $\varepsilon_1' \times (\hbar\omega)^2$ spectra exhibit a gradual decrease in value with photon energy, intersecting the zero line near 2.7–3.5 eV and producing a wide plateau in the visible region. The absorptive peak near 1.3 eV in the $\varepsilon_2' \times (\hbar\omega)^2$ spectrum near 1.3 eV can be

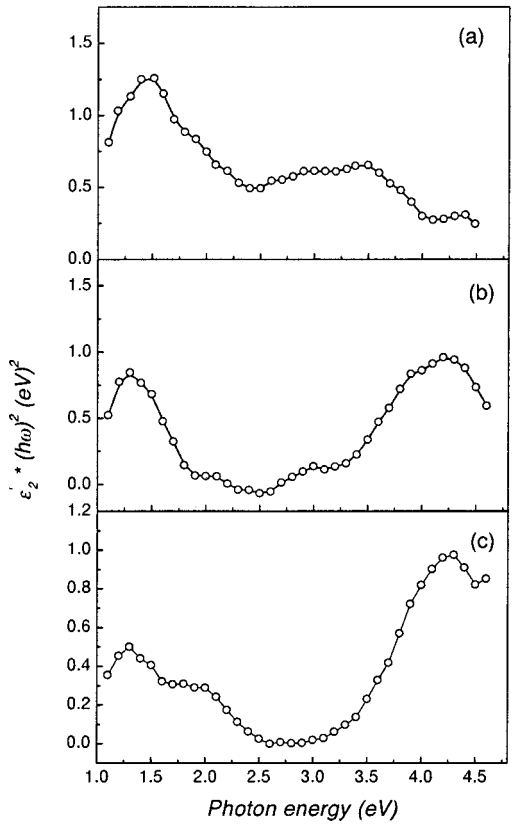

FIG. 10. Extracted $\varepsilon_2' \times (\hbar\omega)^2$ spectra for the spin-polarized Pt sublayers in the Co/Pt MLF (a) sample 3, (b) sample 4, and (c) sample 5, using the simulated results based on the mixed-interface (open circles) model.

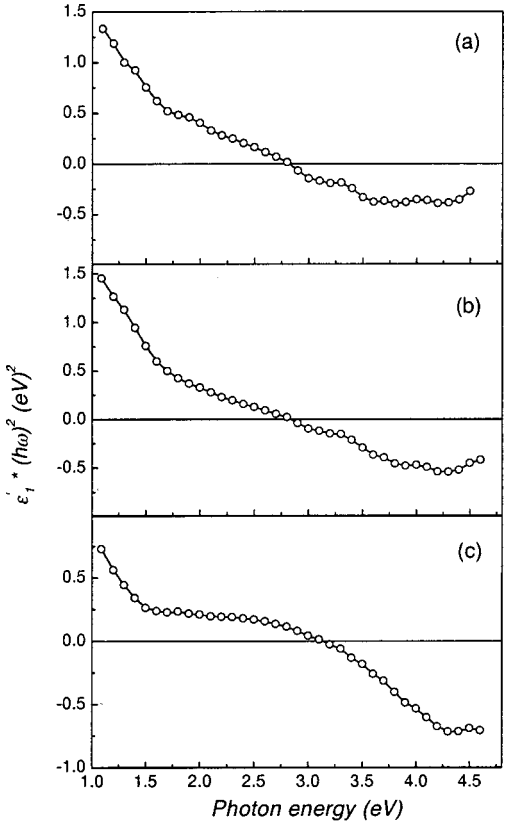

FIG. 11. Extracted $\varepsilon_1' \times (\hbar\omega)^2$ spectra for the spin-polarized Pt sublayers in the Co/Pt MLF (a) sample 3, (b) sample 4, and (c) sample 5, using the simulated results based on the mixed-interface (open circles) model.

considered as unexpected, because no prominent feature is observed around this energy in the experimental EKE spectra of the investigated Co/Pt MLF. On the other hand, such a behavior can be understood when we remind the significant growth of the σ (and hence ε_2) and ε_1 with a decrease in photon energy for the Pt film. Then, according to Eq. (23), the MO response decreases with the increase in ε_2 and ε_1.

The results in Figs. 10 and 11 also reveal a dependence on the input data, i.e., on sample. All the spectra obtained with the mixed interfaces show a lower magnitude than those with the sharp interfaces, even though both spectral shapes are similar. Such a behavior of the $\varepsilon_2' \times (\hbar\omega)^2$ spectra is clear: the smaller quantity of the MO-active media, the lower MO response.

The dependence on the input data can be can be understood by taking into account the results of the first-principles theoretical calculations of the MO properties of the Co/Pt MLF and Co_xPt_{1-x} alloys.[5,34] These calculated MO properties show a prominent dependence on structural and chemical ordering. The microscopic origin for the extracted absorption peaks related to the spin-polarized Pt can be explained further by the first-principles calculations for the MO effects of Pt.

IV. CONCLUSIONS

(i) The optical and MO properties of the Co/Pt MLF with a nearly constant Pt sublayer thickness and a variable Co sublayer thickness, as well as pure Co, pure Pt, and $Co_{0.51}Pt_{0.49}$ alloy films were investigated. It was shown that the MO response for the $Co_{0.51}Pt_{0.49}$ alloy film is higher with respect to the Co/Pt MLF with corresponding composition.

(ii) It was experimentally revealed that a change in local environment caused by the structural fcc-$L1_0$ transformation in the $Co_{0.51}Pt_{0.49}$ alloy film leads to significant changes in the optical and MO properties of alloy.

(iii) The off-diagonal components of the DF for the Co/Pt MLF (not shown explicitly in this paper) as well as pure Co and $Co_{0.51}Pt_{0.49}$ alloy films were determined.

(iv) The real structures of the Co/Pt MLF were elucidated on the basis of the comparison of their experimental and computer-simulated optical properties.

(v) The MO properties (off-diagonal components of the DF) for the spin-polarized Pt sublayers in the Co/Pt MLF were determined.

(vi) The obtained experimental results were compared with the corresponding theoretical data.

ACKNOWLEDGMENTS

This work was supported by the Korea Science and Engineering Foundation through the Atomic-scale Surface Science Research Center, and Project Nos. 97-0702-01-01-3 and 995-0200-004-2, and also by a Korea Research Foundation Grant (KRF-99-D00048).

[1] D. Weller, W. Reim, K. Spörl, and H. Brändle, J. Magn. Magn. Mater. **93**, 183 (1991).
[2] W.B. Zeper, F.J.A.M. Greidanus, P.F. Carcia, and C.R. Fincher, J. Appl. Phys. **65**, 4971 (1989).
[3] K. Sato, H. Ikekame, Y. Tosaka, K. Tsuzukiyama, Y. Togami, and M. Fujisawa, J. Magn. Magn. Mater. **126**, 572 (1993).
[4] Š. Višnovský, M. Nyvlt, V. Parizek, P. Kielar, V. Prosser, and R. Krishnan, IEEE Trans. Magn. **MAG-29**, 3390 (1993).
[5] S. Uba, L. Uba, A.N. Yaresko, A.Ya. Perlov, V.N. Antonov, and R. Gontarz, Phys. Rev. B **53**, 6526 (1996).
[6] E.R. Moog, J. Zak, and S.D. Bader, J. Appl. Phys. **69**, 880 (1991).
[7] T. Sato, Y. Tosaka, Horoshi Ikeme, M. Watanabe, K. Takanashi, and H. Fujimori, J. Magn. Magn. Mater. **148**, 206 (1995).
[8] J. Ferre, M. Nývlt, G. Pennisard, V. Prosser, D. Renard, and Š. Višnovský, J. Magn. Magn. Mater. **148**, 281 (1995).
[9] A. Yamaguchi, S. Iwata, S. Tsunashima, and S. Ushiyama, J. Magn. Magn. Mater. **121**, 542 (1993).
[10] R. Atkinson, S. Pahirathan, I.W. Salter, and P.J. Walker, J. Magn. Magn. Mater. **130**, 442 (1994).
[11] T. Katayama, W. Geerts, Y. Suzuki, D. Fujitani, and N. Okuzawa, J. Magn. Magn. Mater. **156**, 171 (1996).
[12] Y. Suzuki, T. Katayama, S. Yoshida, and K. Tanaka, Phys. Rev. Lett. **68**, 3355 (1992).
[13] Y.V. Kudryavtsev, A.Y. Kucherenko, J. Dubowik, F. Stobiecki, and Y.P. Lee, J. Vac. Sci. Technol. A **16**, 389 (1998).
[14] Y.P. Lee, G.M. Lee, K.W. Kim, Y.V. Kudryavtsev, and L. Smardz, J. Magn. Soc. Jpn. **23**, 361 (1999).
[15] R. Atkinson and P.M. Dodd, J. Magn. Magn. Mater. **173**, 202 (1997).
[16] C.Y. You, S.C. Shin, and S.Y. Kim, Phys. Rev. B **55**, 5953 (1997).
[17] M. Angelakeris, P. Poulopoulos, N.K. Flevaris, R. Knapek, M. Nývlt, V. Prosser, and Š. Višnovský, J. Magn. Magn. Mater. **140-144**, 579 (1995).
[18] J.A.C. Bland, R.P. Cowburn, J. Ferré, J.S. Gray, R. Lopušník, M. Nývlt, V. Prosser, R. Urban, and Š. Višnovský, J. Magn. Magn. Mater. **156**, 177 (1996).
[19] R. Gontarz, T. Lucinski, L. Uba, S. Uba, and Y.V. Kudryavtsev, Acta Phys. Pol. A **85**, 427 (1994).
[20] J.R. Beattie and G.M. Conn, Philos. Mag. **46**, 235 (1955).
[21] G. S. Krinchik, *Physics of Magnetic Phenomena* (MGU, Moscow, 1976) (in Russian).
[22] R.M.A. Azzam and N.M. Bashara, *Ellipsometry and Polarized Light* (North-Holland, Amsterdam, 1977).
[23] G.S. Krinchik and V.A. Artemév, Zh. Éksp. Teor. Fiz. **53**, 1901 (1967) [Sov. Phys. JETP **26**, 1080 (1968)].
[24] L.V. Nikitin, E.V. Likhushina, S.V. Sveshnikov, and G.V. Smirnitskaya, J. Magn. Magn. Mater. **148**, 102 (1995).
[25] M.M. Kirillova, G.A. Bolotin, and L.V. Nomerovannaya, Opt. Spectrosk. **49**, 742 (1980) [Opt. Spectrosc. **49**, 406 (1980)].
[26] J. Rivory and B. Bouchet, J. Phys. F: Met. Phys. **9**, 327 (1979).
[27] M.M. Kirillova, L.V. Nomerovannaya, and M.M. Noskov, Phys. Met. Metallogr. **34**, 60 (1972) (in Russian).
[28] J.H. Weaver, Phys. Rev. B **11**, 1416 (1975).
[29] Yu.A. Uspenskij and S.V. Khalilov, Zh. Éksp. Teor. Fiz. **95**, 1022 (1989) [Sov. Phys. JETP **68**, 588 (1989)].
[30] P.G. van Engen, K.H.J. Buschow, R. Jongebreur, and M. Erman, Appl. Phys. Lett. **42**, 202 (1983).
[31] D. Weller, G.R. Harp, R.F.C. Farrow, A. Cebollada, and J. Sticht, Phys. Rev. Lett. **72**, 2097 (1994).
[32] R.M. Osgood III, K.T. Riggs, A.E. Johnson, J.E. Mattson, C.H. Sowers, and S.D. Bader, Phys. Rev. B **56**, 2627 (1997).
[33] G.Y. Guo and H. Ebert, Phys. Rev. B **50**, 10 377 (1994).
[34] G.Y. Guo and H. Ebert, Phys. Rev. B **51**, 12 633 (1995).
[35] Ya. Perlov, H. Ebert, A.N. Yaresko, V.N. Antonov, and D. Weller, Solid State Commun. **105**, 273 (1998).
[36] A. Cebollada, D. Weller, J. Sticht, G.R. Harp, R.F.C. Farrow, R.F. Marks, R. Savoy, and J.C. Scott, Phys. Rev. B **50**, 3419 (1994).
[37] S. Uba, A.N. Yaresko, L. Uba, A.Ya. Perlov, V.N. Antonov, R. Gontarz, and H. Ebert, Phys. Rev. B **57**, 1534 (1998).
[38] W.P. Van Drent and T. Suzuki, J. Magn. Magn. Mater. **175**, 53 (1997).